

LASER ABLATION ION SOURCE FOR HIGHLY CHARGE-STATE ION BEAMS

Naoya Munemoto^{#, A, B}, Naoto Takakura^C, Susumu Takano^B, Isao Yamane^B,
Ken Takayama^{A, B, D, E}

^{A)} Tokyo institute of Technology, Nagatsuta, Kanagawa, Japan

^{B)} High Energy Accelerator Research Organization, Tsukuba, Ibaraki, Japan

^{C)} Nagaoka University of Technology, Nagaoka, Niigata, Japan

^{D)} The Graduate University for Advanced Studies, Hayama, Kanagawa, Japan

^{E)} Tokyo City University, Tamatsutsumi, Tokyo, Japan

Abstract

KEK Laser ablation ion source (KEK-LAIS) has been developed to generate highly ionized metal ions and fully ionized carbon ions since 2012. Laser ablation experiment has been carried out by using Nd-YAG laser (838 mJ/pulse, 20 ns) at the KEK test bench. Basic parameters such as momentum spectrum and plasma current have been obtained. Experimental results are compared with the existing results, which had been obtained by Munemoto at BNL. In addition, the newly designed electrostatic analyzer and a plan of the future experiment are discussed.

INTRODUCTION

The High Energy Accelerator Research Organization Digital Accelerator (KEK-DA) is a 10 Hz fast-cycling induction synchrotron without a large-scale injector [1]. The KEK-DA is capable of accelerating any species of ion, regardless of its possible charge state. At this moment, low-charge-state gaseous ions are provided from the X-band ECRIS [2], which is installed in the high-voltage platform.

Induction synchrotron was proposed as an alternative to a RF synchrotron. Recently an ideal induction synchrotron has been designed as a hadron driver for cancer therapies [3]. It does not use a conventional injector system consisting of RFQ, DTL, and carbon stripper foil. It is indispensable to produce full-stripped carbon ions in the ion source. Demonstration of such an ion source is strongly demanded.

The laser abrasion ion source (LAIS) has been developed at KEK since 2012, as a method to easily produce highly charged ions at low cost. R&D works on the LAIS to produce high intensity ion beam is going on based on preceding studies [4]. Plasma in the LAIS is produced as a result of interaction between the laser and a target substance, and drifts downstream to the extraction region, where an ion beam is extracted from the plasma by applying a few tens kV across the acceleration gap.

Laser irradiation on the graphite target was tried at BNL by using two laser systems of Quantel Brilliant b (1064 nm, $\tau=6$ ns, $E=750$ mJ) and Ekspla (1064 nm,

$\tau=150 \sim 550$ ps, $E=500$ mJ) in 2013. Then a similar ion source test bench employing the Spectron SL800 was constructed at KEK in 2014 and the laser irradiation experiment has been conducted. Its first priority is to reproduce the experiment results obtained at BNL and to acquire further information.

Comparison between the existing experimental results and recent results newly obtained at the test bench of the KEK-LAIS is discussed here.

EXPERIMENTAL SETUP

Layout of the KEK-DA LAIS Chamber is depicted in Fig. 1. The chamber consists of the optical components and target unit. Graphite (IG-110) is used as a target material, which has the density of 1.77 g/cm^3 , the homogeneous fine grain structure, and 5 mm in thickness. The maximum laser irradiation area on the target is 169 cm^2 . All of optical components are located inside the chamber. The laser beam is guided into the chamber through the anti-reflection coated BK7 window ($\phi 40$ mm), reflected by the coated mirror ($\phi 30$ mm), and delivered to the focusing lens ($\phi 25$ mm, $f=200$ mm). Spot size on the target is controlled by adjusting the focusing lens position so as to minimize the TOF of plasma from the target to the Faraday cup (FC) (see Fig. 1). In the other ward, the laser focusing parameter is determined so that the observed velocities of particle become maximum. The laser has an incident angle of 30° against the target surface. These optical components are securely protected from vapor contamination from the target by the thin aluminum shielding. Schematic of the KEK-LAIS test bench is depicted in Fig. 2, where LAIS chamber, solenoid guide system, FC measuring system, and static electric analyzer are shown.

Vacuum of plasma chamber and FC chamber are 2×10^{-4} Pa and 2.5×10^{-5} Pa, respectively. Spectron Laser system SL800 Nd-YAG laser ($\lambda=1064$ nm, $\tau=20$ ns, $E=838$ mJ) is used. If its laser profile is assumed to be Gaussian, the spot size and energy density can be calculated using following formula [5]:

#munemoto.n.ad@m.titech.ac.jp

$$d_0 \approx M^2 \frac{2f\lambda}{D}$$

$$I_0 = \frac{2P}{\pi d_0^2}$$

d_0 : spot diameter, f : focus distance, λ : wavelength,
 D : incident beam diameter

I_0 : Laser power density, P : Laser power, M^2 : Gaussian beam=1

The focused laser power density is about 1.42×10^{13} W/cm² in an ideal condition. To obtain reproducible carbon ion beams, the irradiated surface is refreshed by moving the X-Y stage by 1mm per shot. The time constant of the FC is $\tau=0.1$ μ s. The aperture of the FC is 1 cm in diameter, and the bias voltage applied to the FC is -50 V. The distance from the target to the FC is 2.6 m. As the trigger signal to measure a FC current, an output signal from the PIN photo diode (Cutoff frequency = 200-300 MHz) observing scattered laser light is used.

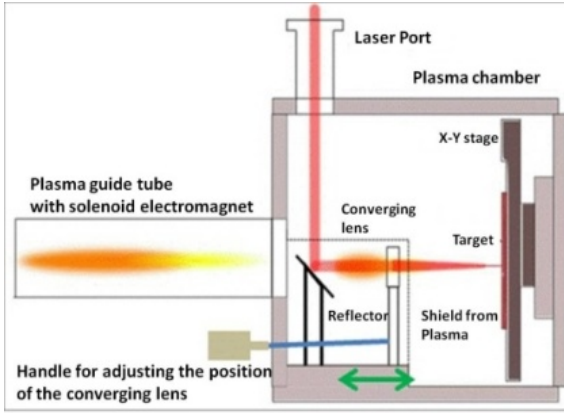


Figure 1: KEK LAIS plasma chamber layout.

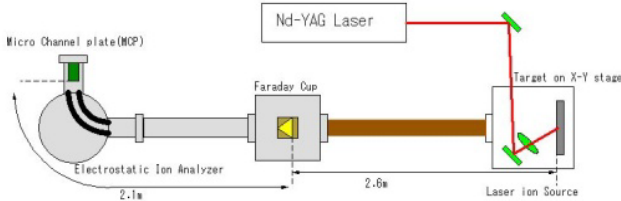


Figure 2: Set-up of the KEK LAIS experiment.

EXPERIMENTAL RESULTS

Analytical Method

Obtained data are scaled to a value at the distance of 1m from the target using following relation,

$$T \sim L \quad (3)$$

$$N \sim 1/L^2 \quad (4)$$

$$I \sim 1/L^3 \quad (5)$$

T is time of flight from the target to the FC, N is number of particle, I is beam current, L is distance between the target to the FC.

Results and Discussion

Table 1 is summarized in the obtained laser plasma parameter. Figure 3 shows the current density as a function of the drift energy, which is measured by the FC. Here, the drift energy is expressed by the following equation.

$$E_{Drift} = \frac{A}{2} mc^2 \frac{1}{c^2} \left(\frac{L}{T} \right)^2 = \frac{A}{2} mc^2 \beta^2 \quad (6)$$

A : Mass number, mc^2 : 939[MeV], c : Light speed,

L : Distance from the target to the Faraday cup,

T : Time of flight, β : Relativistic beta

$$T_e[eV] = 100 \left(\frac{\bar{Z}P[GW]}{d[mm]} \right)^2 \quad (7)$$

$$E_{kin}^{max} \approx \frac{15}{2} (Z+1) T_e[eV] \quad (8)$$

T_e : Electron temperature, Z : Charge state, \bar{Z} : Averaged charge state,
 d : spot size, P : Laser power

Substituting the experimentally obtained largest drift energy into Eq. (8), we have the plasma temperature T_i . Substitution of this T_i into Eq. (7) gives the spot size of 223 μ m [6]. Meanwhile, the spot size derived from Eq. (1) is 19.4 [μ m]. We find a fact that the factor M^2 is around 11 and the laser is not focused at its focal point as expected.

The experimental results obtained at KEK and BNL are summarized together in Figs. 4 and 5, where the maximum drift energy and the current density are given as functions of the laser power, respectively. From Fig. 4 we know that the larger the laser power, the higher plasma energy is obtained. However, the plasma energy decreases beyond 1 TW. This region of the laser power density is outside the region where classical absorption is dominant and close to the region where non-linear forces appear [7, 8]. It is found in Fig.5 that the current density decreases below 100 GW in contract to our expectation. This may be attributed to the fact that the laser of 850[mJ] 20[ns] employed at KEK is not well focused and the produced plasma is not sufficiently ionized.

Table 1: The Obtained Laser Plasma Parameter

Max plasma current density	18.8 [mA/cm ²]
Fastest arriving time	3.28 [μ s]
Fastest drift energy	5.72[keV]
Pulse width(half width)	0.85 [μ s]
Drift energy of centre	3.57 [keV]
Half width of drift energy	+1.05~-0.56 [keV]

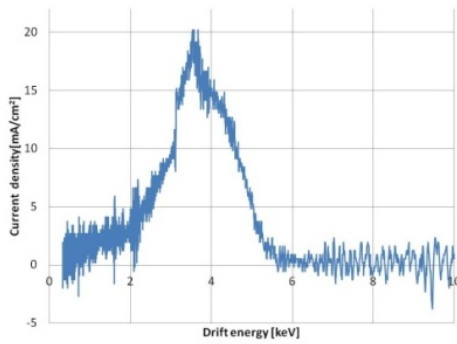


Figure 3: Current density vs. Drift energy (KEK LAIS).

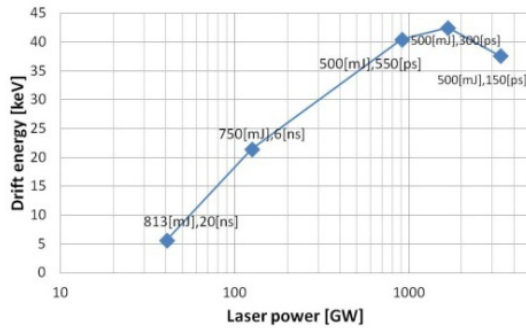


Figure 4: Drift energy vs. Laser power.

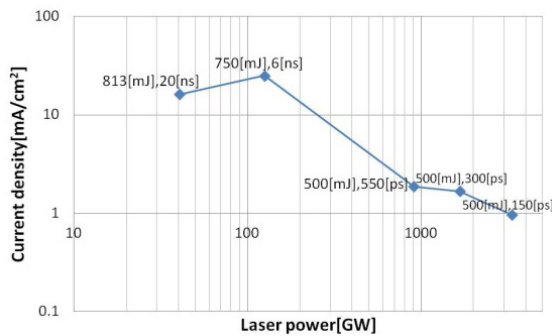


Figure 5: Current density vs. Laser power.

DEVELOPMENT OF ELECTROSTATIC ANALYZER

Figure 6 shows the newly designed electrostatic analyzer, which is used to obtain the charge-state spectrum with a good accuracy. Two 90 degree electrode plates with the radius of 15.3 cm and 15.8 cm are placed in parallel. Slit plates are placed at the entrance and exit of the parallel plate region (at 5 mm upstream and 5 mm downstream). Their aperture is 0.5 mm in the transverse direction and 5 mm in the vertical direction. The simulation software CST has been used for analysing the performance of the electrostatic analyzer system. Orbits of Carbon 6+ macro particles 10,000, which have a energy spread of 10 % and a tilt in the moving direction of 20 degrees, were tracked under the 3D entire field distribution.

The centre energy of a fraction of macro particles that can propagate through the downstream slit is determined by the following equation,

$$V_2 - V_1 = 2 \left(\ln \frac{R_2}{R_1} \right) \frac{T}{Z} \tag{9}$$

V_i : Voltage applied to the electrode plate

R_i : The radius of the electrode

T : Drift energy of plasma, Z : Charge state

It is found in Fig. 7 that the simulation result with respect to the analyzed average energy agrees with the analytical solution well. The energy resolution was within 2 % (see Fig. 8).

FUTURE PLAN

- Analysis of the charge state distribution using the electrostatic analyser discussed here.
- Emittance measurement.
- Optimization of the solenoid magnetic field applied to the laser plasma.
- Pre-acceleration with 20 kV, post-acceleration with 180 kV, beam transport thorough the LEBT, and injection into the KEK-DA.

CONCLUSION

The Laser ablation experiment using the laser SL-800 has been carried out and their results have been compared with the existing results. It turns out that the obtained plasma is not sufficiently heated, because the laser pulse is too long. Numerical simulations to confirm the operational performance of the assembled electrostatic analyzer has been done. They suggest that our electrostatic analyzer will work as expected.

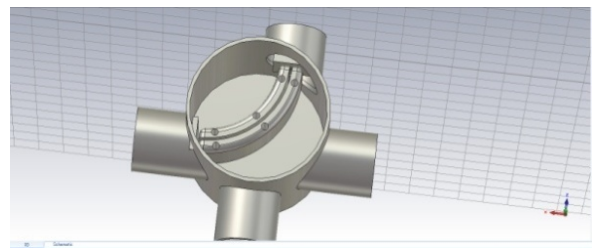


Figure 6: Simulation model of the electrostatic analyzer.

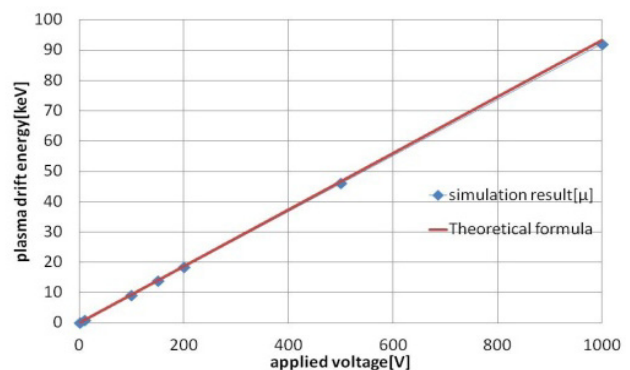


Figure 7: Averaged drift energy vs. Applied voltage.

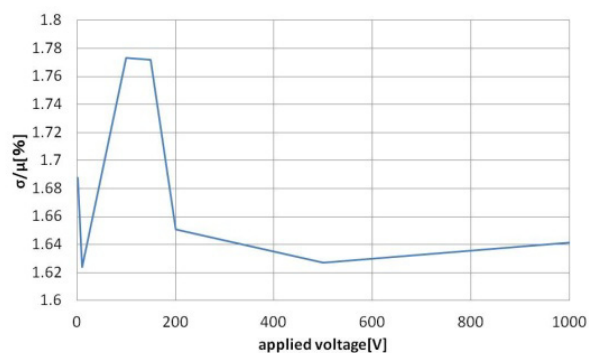


Figure 8: Beam resolution vs. Applied voltage.

REFERENCES

- [1] K.Takayama *et al.*, *Phys. Rev. ST-AB* **17**, 010101 (2014).
- [2] Leo Kwee Wah et al., in *Proceedings of ECRIS2010*, August 23-26, 2010 Grenoble, France, TUPOT15.
- [3] Leo Kwee Wah et al. submitted to *Phys. Rev. ST-AB* (2015).
- [4] N.Munemoto et al., *Rev. Sci. Inst.* **85**, 02B922 (2014)
- [5] A. E, Siegman *LASERS* Sec17.2 .
- [6] I. V. Roudskoy *Laser and Particle Beams* **14**, 369 (1996).
- [7] P.Mora *Phys.Fluids*, **25**,1051(1982).
- [8] L. Láska et al., *Appl. Phys. Lett.* **86**, 081502 (2005).